

Atomic picture of structural relaxation in silicate glasses

Cite as: Appl. Phys. Lett. **114**, 233703 (2019); <https://doi.org/10.1063/1.5095529>

Submitted: 10 March 2019 . Accepted: 30 May 2019 . Published Online: 12 June 2019

Weiying Song, Xin Li, Bu Wang , N. M. Anoop Krishnan , Sushmit Goyal, Morten M. Smedskjaer, John C. Mauro , Christian G. Hoover, and Mathieu Bauchy 



[View Online](#)



[Export Citation](#)



[CrossMark](#)

ARTICLES YOU MAY BE INTERESTED IN

[Meandering growth of in-plane silicon nanowire springs](#)

Applied Physics Letters **114**, 233103 (2019); <https://doi.org/10.1063/1.5097429>

[Solid state MXene based electrostatic fractional capacitors](#)

Applied Physics Letters **114**, 232903 (2019); <https://doi.org/10.1063/1.5094236>

[Direct evidence of Mg diffusion through threading mixed dislocations in GaN p-n diodes and its effect on reverse leakage current](#)

Applied Physics Letters **114**, 232105 (2019); <https://doi.org/10.1063/1.5097767>

Applied Physics Letters

Mid-IR and THz frequency combs
special collection

[Read Now!](#)



Atomic picture of structural relaxation in silicate glasses

Cite as: Appl. Phys. Lett. 114, 233703 (2019); doi: 10.1063/1.5095529

Submitted: 10 March 2019 · Accepted: 30 May 2019 ·

Published Online: 12 June 2019



View Online



Export Citation



CrossMark

Weiying Song,¹ Xin Li,¹ Bu Wang,^{1,2} N. M. Anoop Krishnan,^{1,3} Sushmit Goyal,⁴ Morten M. Smedskjaer,⁵ John C. Mauro,⁶ Christian G. Hoover,⁷ and Mathieu Bauchy^{1,a)}

AFFILIATIONS

¹Physics of Amorphous and Inorganic Solids Laboratory (PARISlab), Department of Civil and Environmental Engineering, University of California, Los Angeles, California 90095, USA

²Department of Civil and Environmental Engineering, University of Wisconsin-Madison, Madison, Wisconsin 53706, USA

³Department of Civil Engineering, Indian Institute of Technology Delhi, Hauz Khas, New Delhi 110016, India

⁴Science and Technology Division, Corning Incorporated, Corning, New York 14831, USA

⁵Department of Chemistry and Bioscience, Aalborg University, 9220 Aalborg, Denmark

⁶Department of Materials Science and Engineering, The Pennsylvania State University, University Park, Pennsylvania 16802, USA

⁷School of Sustainable Engineering and the Built Environment, Arizona State University, Tempe, Arizona 85287, USA

^{a)}Electronic mail: bauchy@ucla.edu. URL: <http://www.lab-paris.com>

ABSTRACT

As nonequilibrium materials, glasses continually relax toward the supercooled liquid state. However, the atomic-scale origin and mechanism of glass relaxation remain unclear. Here, based on molecular dynamics simulations of sodium silicate glasses quenched with varying cooling rates, we show that structural relaxation occurs through the transformation of small silicate rings into larger ones. We demonstrate that this mechanism is driven by the fact that small rings (<6-membered) are topologically overconstrained and experience some internal stress. At the atomic level, such stress manifests itself by a competition between radial and angular constraints, wherein the weaker bond-bending constraints yield to the stronger bond-stretching ones. These results strongly echo von Neumann's $N - 6$ rule in grain growth theory and suggest that the stability of both atomic rings and two-dimensional crystal grains is fully topological in nature.

Published under license by AIP Publishing. <https://doi.org/10.1063/1.5095529>

If cooled fast enough, the crystallization of a liquid can be avoided.¹ As temperature becomes lower than the melting temperature, the system accesses the metastable supercooled liquid state.² The relaxation time τ of the system then dramatically increases with decreasing temperature. At some point, τ exceeds the observation time and the system becomes an out-of-equilibrium glass, which slowly relaxes toward the metastable supercooled liquid state.^{3,4} Despite its fundamental and technical relevance,^{5–7} the atomic nature and origin of glass relaxation remain poorly understood.^{8–12} Various structural signatures of glass relaxation and aging have been observed, including changes in interatomic angles,^{13–16} local connectivity,^{17,18} chain size distribution,¹⁹ etc. To this end, atomistic simulations have been key to reveal some atomic details that are largely invisible to conventional experiments.^{20,21} However, although many studies have been devoted to “model glasses”—e.g., Lennard-Jones (LJ) glasses^{22–27}—the atomic mechanism of relaxation in more industry-relevant silicate glasses remains far less understood.²⁸

Here, to examine the atomic manifestation and driving force for glass relaxation, we investigate by molecular dynamics (MD) simulations the structure of a series of sodium silicate glasses $(\text{Na}_2\text{O})_{30}(\text{SiO}_2)_{70}$ (mol. %)—an archetypical model for modified silicate glasses—prepared with varying cooling rates. Configurations made of 3000 atoms are initially created by randomly placing the atoms in a cubic box while ensuring the absence of any unrealistic overlap. The systems are then equilibrated at 5000 K in the isothermal-isobaric (NPT) ensemble for 1 ns at zero pressure to ensure the loss of the memory of the initial configuration. The glasses are finally formed by linearly cooling the liquids from 5000 to 0 K in the NPT ensemble at zero pressure and with a cooling rate ranging from 10^2 to 10^{-3} K/fs. Note that the slowest cooling rate used herein corresponds to a total simulation time of about 5 μ s, which is the slowest cooling rate ever used in direct MD simulations of silicate glasses.^{15,29} All MD simulations are performed with the LAMMPS package,³⁰ using the well-established Teter potential³¹ with an integration timestep of 1 fs. The short-range interaction

cutoff is chosen as 8.0 \AA , and Coulomb interactions are evaluated by the Ewald summation method with a cutoff of 12 \AA .³¹

Figure 1 shows the evolution of the enthalpy and molar volume of the glass (at 0 K) as a function of the cooling rate. As expected, we observe that the glass enthalpy decreases with the decreasing cooling rate, which indicates that, as the simulation time increases, the glass can relax toward a more stable configuration. We also note that the molar volume of glass also decreases with the decreasing cooling rate, which shows that relaxation results in a more compact glass. As shown in Fig. 1, the dependence on the cooling rate γ of both the enthalpy H and molar volume V_m can be well described by a power law, as predicted by mode-coupling theory²³

$$H(\gamma) = H(\gamma = 0) + (A\gamma)^{1/\delta}, \quad (1)$$

where A and δ are some fitting parameters and $H(\gamma = 0)$ is the value of the property (here, enthalpy) that would be achieved for a (fictitious) zero cooling rate. We find here $\delta = 3.7$ and 2.2 for the enthalpy and molar volume, respectively, which suggests that the relaxation mechanisms governing these quantities have some degree of decorrelation from each other.^{14,20,21}

We now focus on investigating the structural signatures of glass relaxation. Various structural quantities are here found to be affected by the cooling rate, including the interatomic angles and the medium-range order (MRO)—a thorough analysis of the effect of the cooling rate on the structure of the sodium silicate glass simulated herein can be found in Ref. 14. Overall, we find that, although the short-range order structure remains weakly affected by the cooling rate, the medium-range order (MRO) structure exhibits some significant variations. This differs from what is observed in metallic glasses, wherein relaxation is associated with some reorganization of the short-range order.³² In silicate glasses, the MRO mostly depends on the silicate ring size distribution, wherein a ring is defined as a shortest closed path within the Si-O network—its size being given by the number of Si atoms belonging to the ring.³³

Figure 2 shows the ring size distribution obtained for the two extreme cooling rates (computed with the RINGS package³⁴). We find that the ring size exhibits a broad distribution centered between 5- and 6-membered rings, in line with previous studies.³⁵ Overall, we observe that the fraction of small rings (defined here as strictly smaller than

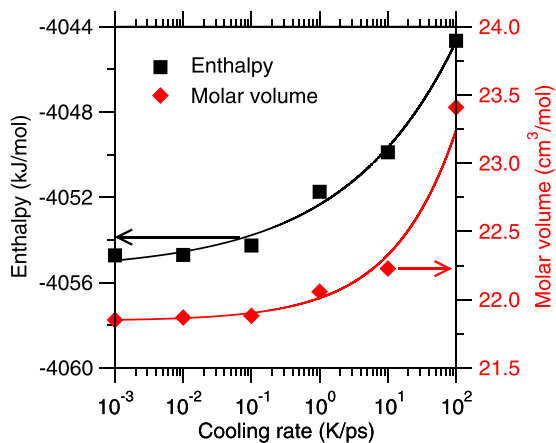


FIG. 1. Enthalpy and molar volume of sodium silicate glasses at 0 K as a function of the cooling rate. The lines are power-law fits [see Eq. (1)].

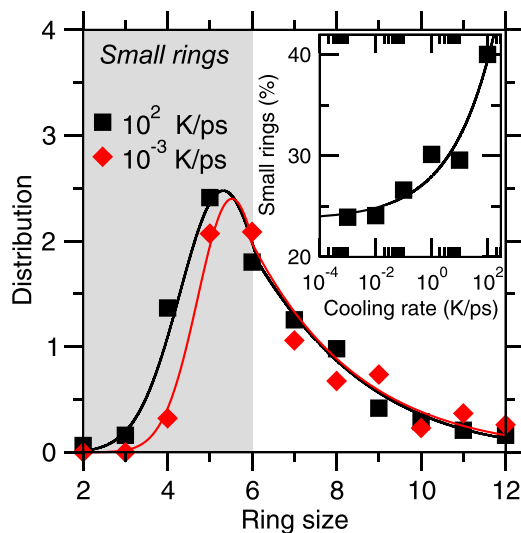


FIG. 2. Silicate ring size distributions of sodium silicate glasses for selected cooling rates. The lines are guides to the eye. The gray area highlights the small overconstrained rings (<6-membered). The inset shows the fraction of such small rings as a function of the cooling rate. The line is a power-law fit [see Eq. (1)].

6-membered) tends to decrease with the decreasing cooling rate (see the inset of Fig. 2), whereas the fraction of larger rings (6-membered and larger) tends to increase. This indicates that, at the atomic level, glass relaxation manifests itself by a transformation of small rings into larger ones, as previously observed in glassy silica.¹³ As shown in the inset of Fig. 2, the cooling rate dependence of the fraction of small rings follows a power law function [see Eq. (1)]. We obtain here $\delta = 3.6$, that is, a power law exponent that is very close to the one obtained for the enthalpy ($\delta = 3.7$). This suggests that the transformation of small into larger rings controls enthalpy relaxation in glasses.

We now investigate the nature of the driving force behind the transformation of small into larger rings upon glass relaxation. We propose here that this mechanism is driven by the fact that small rings experience some internal stress, which gets released upon transformation into a larger ring. The mechanical stability of rings can be elegantly described within the framework of topological constraint theory,^{36,37} wherein the stability of a ring depends on the balance between internal degrees of freedom and internal constraints. Here, we consider the SiO_4 units to be some rigid structures and only consider their mutual connectivity. The stability of an N -membered ring can then be determined as follows. Starting from the initial $3N$ degrees of freedom offered by each node, each node of the ring creates 1 bond-stretching (BS) constraint (which fixes the distance between the node and its two neighbors—note that BS constraint is shared between 2 nodes) and 1 bond-bending (BB) constraint (which fixes the angle between the node and its two neighbors). The number of remaining internal degrees of freedom F (or floppy modes) of an N -membered ring is then given by

$$F = 3N - N - N - 6 = N - 6, \quad (2)$$

where 6 is the number of rigid-body degrees of freedom of the ring. This simply means that a triangle (i.e., 3-membered ring) with fixed edges and angles is overconstrained and exhibits 3 redundant

constraints (i.e., $F = -3$).³⁸ Overall, this enumeration shows that N -membered rings are stressed-rigid (i.e., overconstrained, $F < 0$), flexible (i.e., floppy, $F > 0$), and isostatic (i.e., optimally constrained, $F = 0$) when N is smaller, larger, or equal to 6. Specifically, this suggests that small rings (less than 6-membered) are under internal stress since all the constraints cannot be satisfied at the same time—so that the weaker constraints (most likely the angular BB constraints) have to yield to the stronger ones (the radial BS constraints).³⁹

To establish this picture, we now rely on the concept of “stress per atom” to assess the mechanical stability of each ring in the network. Although stress can only be meaningfully defined at the macroscopic scale, we adopt here the formalism proposed by Egami.⁴⁰ To this end, we compute the contribution of each atom to the virial of the system and divide this term by the Voronoi volume of the atom.⁴⁰ This defines an atomic stress tensor comprising 6 independent components (3 normal stresses σ_{xx} and 3 shear stress $\tau_{\alpha\beta}$), where the indexes α and β denote the direction x , y , or z . We then calculate for each atom the hydrostatic stress σ as the trace of the stress tensor

$$\sigma = \frac{1}{3} (\sigma_{xx} + \sigma_{yy} + \sigma_{zz}) \quad (3)$$

and the von Mises shear stress τ as

$$\tau = \frac{1}{3} \sqrt{\tau_{xy}^2 + \tau_{xz}^2 + \tau_{yz}^2}. \quad (4)$$

Note that, although the network as a whole is at zero pressure, some bonds are under compression while others are under tension—so that they mutually compensate each other. Based on this approach, we find that Si atoms are systematically under local tension (i.e., positive hydrostatic stress), whereas O atoms are under compression (i.e., negative hydrostatic stress).

To isolate the contribution of the ring geometry to the stress of each Si atom, the stress per atom calculation is repeated in Q^n clusters ($n = 0-4$) that are fully isolated, that is, with no rings (here, a Q^n unit denotes a SiO_4 tetrahedron that is connected to n other SiO_4 tetrahedra, i.e., with $4-n$ terminating O atoms). The isolated clusters are prepared by placing the atoms as perfect SiO_4 tetrahedra, charge-balancing the terminating O atoms by Na cations, and performing an energy minimization—prior to the stress calculation. Finally, for each Si atom, we define the hydrostatic and shear “internal stresses” as the difference between the hydrostatic and von Mises shear stresses exhibited in the network and those experienced in isolated clusters (ensuring a consistent Q^n state in network and isolated clusters).

Figure 3 shows the average values of the internal hydrostatic stress and von Mises shear stress per Si atom as a function of the cooling rate. We observe that both the average hydrostatic and shear stresses decrease upon relaxation. Notably, the internal shear stress nearly vanishes at a low cooling rate. This suggests that glass relaxation is largely governed by the release of some atomic-level hydrostatic and shear stress initially present in the network.

We now investigate the relationship between atomic stress and ring size distribution. Figure 4 shows the average internal hydrostatic stress per Si atom as a function of the size of the smallest ring it belongs to. We first note that large rings (i.e., 6-membered and larger) do not experience any noticeable internal hydrostatic stress. In contrast, small rings (i.e., smaller than 6-membered) exhibit some significant internal hydrostatic stress, which is found to increase linearly with the number

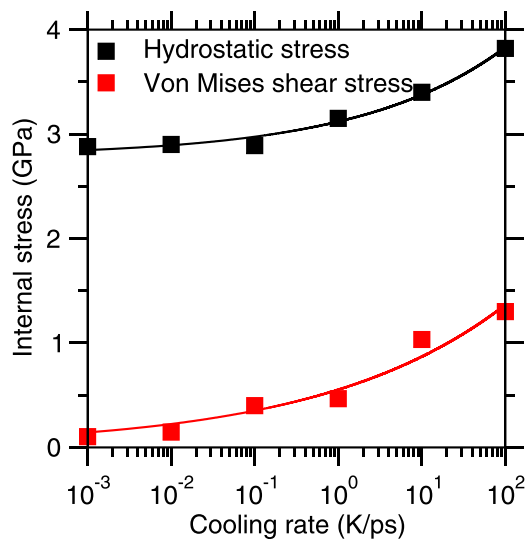


FIG. 3. Average internal hydrostatic and von Mises shear stresses per Si as a function of the cooling rate. The lines are power-law fits [see Eq. (1)].

of redundant constraints. Note that the results presented herein correspond to a sodium silicate glass cooled at 100 K/ps, as such a high cooling rate yields a large number of small rings and, thereby, improves the statistics of the data (see Fig. 2). However, we note that the stress vs ring size curve does not significantly depend on the cooling rate—but the decrease in the fraction of small rings upon a slower cooling rate (see Fig. 2) results in a decrease in the overall stress experienced by the Si atoms present within the glass network (see Fig. 3). Overall, these

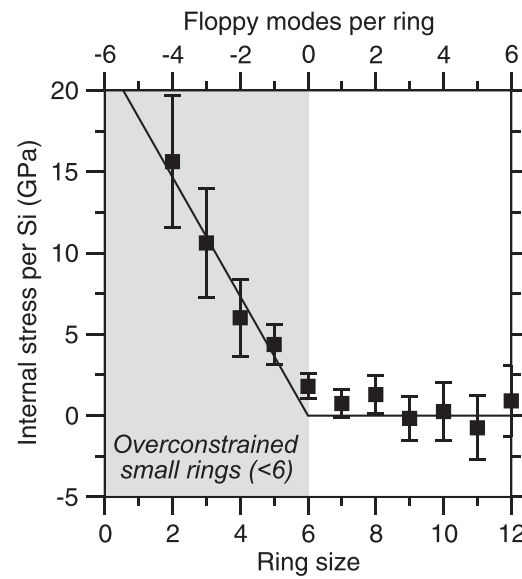


FIG. 4. Average internal hydrostatic stress per Si in a sodium silicate glass cooled at 100 K/ps as a function of the size of the smallest ring it belongs to. The number of floppy modes per ring is also indicated [see Eq. (2)]. The line is a guide to the eye. The gray area highlights the small overconstrained rings (<6-membered).

results strongly support the fact that small rings are mechanically unstable and that their existence is the driving force for the structural relaxation of silicate glasses. This picture is consistent with the fact that the equilibrium zero-pressure crystalline forms of SiO_2 (β -cristobalite, α -quartz, and β -tridymite) only exhibit 6- (and 8-) membered rings. Hence, this suggests that the existence of small rings is an intrinsic signature of out-of-equilibrium silicate phases. In contrast, no correlation between the internal shear stress and the ring size is observed, which suggests that the atomic shear stress has a distinct origin.

Interestingly, these results reveal an unexpected analogy between rings in atomic networks and grain sides in polycrystalline systems. Specifically, the mechanical instability of small rings that is demonstrated herein strongly echo von Neumann's $N - 6$ rule, which states that two-dimensional grains comprising fewer than 6 sides are unstable and tend to disappear upon annealing, whereas larger grains tend to grow.⁴¹ Based on von Neumann's analysis, small grains undergo a free energy penalty that is proportional to $6 - N$, which is analogous to Eq. (2) in the case of atomic rings. This shows that the time-evolution of both atomic rings and two-dimensional crystal grains is fully topological in nature.

Finally, we further investigate the structural manifestation of the internal stress exhibited by small rings. As mentioned above, such internal stress arises from the fact that small rings are overconstrained, that is, they exhibit more constraints than degrees of freedom. As such, all the radial and angular constraints cannot be satisfied simultaneously. To reveal the atomic-scale manifestation of the competition between radial and angular constraints, we compute the average Si-O bond length and the average Si-O-Si and O-Si-O angles as a function of the smallest ring size these units belong to. We first observe that the average Si-O bond length remains largely unaffected by the ring size (less than 1% variation, not shown here). In contrast, both the average Si-O-Si and O-Si-O angles strongly depend on the ring size (see Fig. 5). In

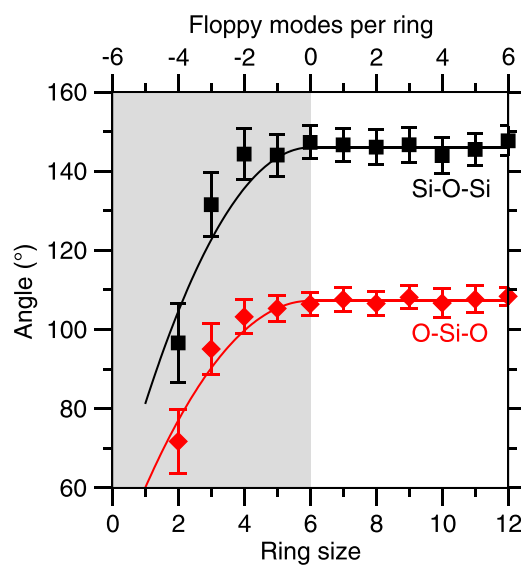


FIG. 5. Average Si-O-Si and O-Si-O angle in a sodium silicate glass cooled at 100 K/ps as a function of the size of the smallest ring it belongs to. The number of floppy modes per ring is also indicated [see Eq. (2)]. The line is a guide to the eye. The gray area highlights the small overconstrained rings (<6-membered).

detail, we observe that both of these angles are nearly constant in large rings (around 107° and 146° for the O-Si-O and Si-O-Si angles, respectively). However, we find that the average values of these angles significantly decrease in smaller rings. This confirms that small rings are strained and that, due to the overconstrained nature of these structures, the weaker angular BB constraints yield to the stronger radial BS constraints. This behavior also exhibits a striking similarity with two-dimensional polycrystalline solids, wherein the average angle at grain junctions drastically decreases in grains comprising fewer than 6 sides.⁴² This further suggests that the mechanical stability of atomic rings and crystal grains shares a common topological origin.

Finally, we discuss the generality of the present results in describing relaxation across different families of glasses. The concept of stress per atom was also used to investigate relaxation in metallic glasses.⁴³ In this class of materials, structural relaxation was described in terms of the mutual annihilation of compressive and tensile structural defects.⁴⁰ This mechanism was also found to explain the low-temperature relaxation of alkali cations in glasses.²¹ In these cases, the atomic stress results from a "radial misfit" between the size of the atom and that of its environment.^{21,40} Such size misfit results in some local volumetric strain energy that drives relaxation. Here, we show that some atomic stress can also form as a consequence of an "angular misfit" in small, overconstrained topological rings, which also acts as a driving force for relaxation. This suggests that the mechanism of relaxation strongly depends on the nature of the interatomic bonds, namely, relaxation is driven by some radial misfit in highly packed metallic phases (which exhibit nondirectional bonds and high coordination numbers), whereas it arises from some angular misfit in more open (ionic)cova-lent phases (which comprise directional bonds and low coordination numbers). This also highlights the fact that the large body of conclusions based on LJ glasses (which do not exhibit directional bonds) may not apply to industrially relevant silicate glasses. Nevertheless, these studies establish the existence of atomic stress as a potentially universal origin of relaxation in out-of-equilibrium glassy phases.

This work was supported by the National Science Foundation under Grants Nos. 1562066, 1762292, 1826420, and 1826050 and by Corning Incorporated through the Glass Age Scholarship.

REFERENCES

- P. G. Debenedetti and F. H. Stillinger, "Supercooled liquids and the glass transition," *Nature* **410**, 259–267 (2001).
- A. K. Varshneya, *Fundamentals of Inorganic Glasses* (Academic Press Inc., 1993).
- E. D. Zanotto and J. C. Mauro, "The glassy state of matter: Its definition and ultimate fate," *J. Non-Cryst. Solids* **471**, 490–495 (2017).
- E. D. Zanotto and D. R. Cassar, "The race within supercooled liquids—Relaxation versus crystallization," *J. Chem. Phys.* **149**, 024503 (2018).
- A. Ellison and I. A. Cornejo, "Glass substrates for liquid crystal displays," *Int. J. Appl. Glass Sci.* **1**, 87–103 (2010).
- G. B. McKenna, "Glass dynamics: Diverging views on glass transition," *Nat. Phys.* **4**, 673 (2008).
- J. C. Phillips, "Stretched exponential relaxation in molecular and electronic glasses," *Rep. Prog. Phys.* **59**, 1133 (1996).
- J. C. Mauro, C. S. Philip, D. J. Vaughn, and M. S. Pambianchi, "Glass science in the United States: Current status and future directions," *Int. J. Appl. Glass Sci.* **5**, 2–15 (2014).
- B. Ruta, G. Baldi, Y. Chushkin, B. Rufflé, L. Cristofolini, A. Fontana, M. Zanatta, and F. Nazzani, "Revealing the fast atomic motion of network glasses," *Nat. Commun.* **5**, 3939 (2014).

¹⁰M. Micoulaut, "Relaxation and physical aging in network glasses: A review," *Rep. Prog. Phys.* **79**, 066504 (2016).

¹¹R. Welch, J. Smith, M. Potuzak, X. Guo, B. Bowden, T. Kiczenski, D. Allan, E. King, A. Ellison, and J. Mauro, "Dynamics of glass relaxation at room temperature," *Phys. Rev. Lett.* **110**, 265901 (2013).

¹²P. Boulchand and B. Goodman, "Glassy materials with enhanced thermal stability," *MRS Bull.* **42**, 23–28 (2017).

¹³K. Vollmayr, W. Kob, and K. Binder, "Cooling-rate effects in amorphous silica: A computer-simulation study," *Phys. Rev. B* **54**, 15808–15827 (1996).

¹⁴X. Li, W. Song, K. Yang, N. M. A. Krishnan, B. Wang, M. M. Smedskjaer, J. C. Mauro, G. Sant, M. Balonis, and M. Bauchy, "Cooling rate effects in sodium silicate glasses: Bridging the gap between molecular dynamics simulations and experiments," *J. Chem. Phys.* **147**, 074501 (2017).

¹⁵J. M. D. Lane, "Cooling rate and stress relaxation in silica melts and glasses via microsecond molecular dynamics," *Phys. Rev. E* **92**, 012320 (2015).

¹⁶S. V. Nemilov and G. P. Johari, "A mechanism for spontaneous relaxation of glass at room temperature," *Philos. Mag.* **83**, 3117–3132 (2003).

¹⁷J. Tan, S. R. Zhao, W. F. Wang, G. Davies, and X. X. Mo, "The effect of cooling rate on the structure of sodium silicate glass," *Mater. Sci. Eng. B-Solid State Mater. Adv. Technol.* **106**, 295–299 (2004).

¹⁸C. Yildirim, J.-Y. Raty, and M. Micoulaut, "Revealing the role of molecular rigidity on the fragility evolution of glass-forming liquids," *Nat. Commun.* **7**, 11086 (2016).

¹⁹S. Dash, P. Chen, and P. Boulchand, "Molecular origin of aging of pure Se glass: Growth of inter-chain structural correlations, network compaction, and partial ordering," *J. Chem. Phys.* **146**, 224506 (2017).

²⁰Y. Yu, M. Wang, D. Zhang, B. Wang, G. Sant, and M. Bauchy, "Stretched exponential relaxation of glasses at low temperature," *Phys. Rev. Lett.* **115**, 165901 (2015).

²¹Y. Yu, M. Wang, M. M. Smedskjaer, J. C. Mauro, G. Sant, and M. Bauchy, "Thermometer effect: Origin of the mixed alkali effect in glass relaxation," *Phys. Rev. Lett.* **119**, 095501 (2017).

²²K. Vollmayr, W. Kob, and K. Binder, "How do the properties of a glass depend on the cooling rate? A computer simulation study of a Lennard-Jones system," *J. Chem. Phys.* **105**, 4714 (1998).

²³W. Kob and H. C. Andersen, "Testing mode-coupling theory for a supercooled binary Lennard-Jones mixture I: The van Hove correlation function," *Phys. Rev. E* **51**, 4626–4641 (1995).

²⁴G. T. Barkema and N. Mousseau, "Event-based relaxation of continuous disordered systems," *Phys. Rev. Lett.* **77**, 4358–4361 (1996).

²⁵N. Mousseau, "Cooperative motion in Lennard-Jones binary mixtures below the glass transition," preprint [arXiv:cond-mat/0004356](https://arxiv.org/abs/cond-mat/0004356) (2000).

²⁶S. S. Schoenholz, E. D. Cubuk, D. M. Sussman, E. Kaxiras, and A. J. Liu, "A structural approach to relaxation in glassy liquids," *Nat. Phys.* **12**, 469–471 (2016).

²⁷S. S. Schoenholz, E. D. Cubuk, E. Kaxiras, and A. J. Liu, "Relationship between local structure and relaxation in out-of-equilibrium glassy systems," *PNAS* **114**, 263–267 (2017).

²⁸K. Vollmayr-Lee, R. Bjorkquist, and L. M. Chambers, "Microscopic picture of aging in SiO_2 ," *Phys. Rev. Lett.* **110**, 017801 (2013).

²⁹H.-B. Yu, R. Richert, and K. Samwer, "Structural rearrangements governing Johari-Goldstein relaxations in metallic glasses," *Sci. Adv.* **3**, e1701577 (2017).

³⁰S. Plimpton, "Fast parallel algorithms for short-range molecular dynamics," *J. Comput. Phys.* **117**, 1–19 (1995).

³¹A. N. Cormack, J. Du, and T. R. Zeitler, "Alkali ion migration mechanisms in silicate glasses probed by molecular dynamics simulations," *Phys. Chem. Chem. Phys.* **4**, 3193–3197 (2002).

³²Y. Q. Cheng and E. Ma, "Atomic-level structure and structure–property relationship in metallic glasses," *Prog. Mater. Sci.* **56**, 379–473 (2011).

³³M. Wang, N. M. A. Krishnan, B. Wang, M. M. Smedskjaer, J. C. Mauro, and M. Bauchy, "A new transferable interatomic potential for molecular dynamics simulations of borosilicate glasses," *J. Non-Cryst. Solids* **498**, 294–304 (2018).

³⁴S. Le Roux and P. Jund, "Ring statistics analysis of topological networks: New approach and application to amorphous GeS_2 and SiO_2 systems," *Comput. Mater. Sci.* **49**, 70–83 (2010).

³⁵J. Du and A. Cormack, "The medium range structure of sodium silicate glasses: A molecular dynamics simulation," *J. Non-Cryst. Solids* **349**, 66–79 (2004).

³⁶J. C. Phillips, "Topology of covalent non-crystalline solids 1: Short-range order in chalcogenide alloys," *J. Non-Cryst. Solids* **34**, 153–181 (1979).

³⁷J. C. Mauro, "Topological constraint theory of glass," *Am. Ceram. Soc. Bull.* **90**, 31–37 (2011).

³⁸M. Micoulaut and J. C. Phillips, "Rings and rigidity transitions in network glasses," *Phys. Rev. B* **67**, 104204 (2003).

³⁹M. Bauchy, M. J. A. Qomi, C. Bichara, F.-J. Ulm, and R. J.-M. Pellenq, "Rigidity transition in materials: Hardness is driven by weak atomic constraints," *Phys. Rev. Lett.* **114**, 125502 (2015).

⁴⁰T. Egami, "Atomic level stresses," *Prog. Mater. Sci.* **56**, 637–653 (2011).

⁴¹J. von Neumann, "Shape of metal grains," *Met. Interfaces* **1952**, 108.

⁴²J. Stavans and J. A. Glazier, "Soap froth revisited: Dynamic scaling in the two-dimensional froth," *Phys. Rev. Lett.* **62**, 1318–1321 (1989).

⁴³V. Vitek and T. Egami, "Atomic level stresses in solids and liquids," *Phys. Status Solidi B* **144**, 145–156 (1987).